



■ BONE BIOLOGY

Parathyroid hormone-related protein exhibits antioxidant features in osteoblastic cells through its N-terminal and osteostatin domains

**S. Portal-Núñez,
J. A. Ardura,
D. Lozano,
I. Martínez de Toda,
M. De la Fuente,
G. Herrero-Beaumont,
R. Largo,
P. Esbrit**

UAM, Madrid, Spain

■ S. Portal-Núñez, PhD, Researcher, Bone and Joint Research Unit,

■ G. Herrero-Beaumont, PhD, Head of Rheumatology Department and Bone and Joint Research Unit,

■ R. Largo, PhD, Senior Researcher, Bone and Joint Research Unit,

■ P. Esbrit, PhD, Emeritus Researcher, Bone and Joint Research Unit, The Institution of Health Research (IIS)-Fundación Jiménez Díaz, UAM, Madrid, Spain.

■ J. A. Ardura, PhD, Researcher and Professor, The Institution of Applied Molecular Medicine (IMMA), Universidad San Pablo CEU Madrid, Spain.

■ D. Lozano, PhD, Researcher, Department of Inorganic and Bioinorganic Chemistry,

■ I. Martínez de Toda, BSc, Predoctoral Student, Animal Physiology II. Faculty of Biology,

■ M. De la Fuente, PhD, Full Professor, Animal Physiology II. Faculty of Biology, Complutense University, Madrid, Spain.

Correspondence should be sent to S. Portal-Núñez; email: sportal@fjd.es

doi: 10.1302/2046-3758.71.BJR-2016-0242.R2

Bone Joint Res 2018;7:58–68.

Objectives

Oxidative stress plays a major role in the onset and progression of involutional osteoporosis. However, classical antioxidants fail to restore osteoblast function. Interestingly, the bone anabolism of parathyroid hormone (PTH) has been shown to be associated with its ability to counteract oxidative stress in osteoblasts. The PTH counterpart in bone, which is the PTH-related protein (PTHrP), displays osteogenic actions through both its N-terminal PTH-like region and the C-terminal domain.

Methods

We examined and compared the antioxidant capacity of PTHrP (1-37) with the C-terminal PTHrP domain comprising the 107-111 epitope (osteostatin) in both murine osteoblastic MC3T3-E1 cells and primary human osteoblastic cells.

Results

We showed that both N- and C-terminal PTHrP peptides at 100 nM decreased reactive oxygen species production and forkhead box protein O activation following hydrogen peroxide (H₂O₂)-induced oxidation, which was related to decreased lipid oxidative damage and caspase-3 activation in these cells. This was associated with their ability to restore the deleterious effects of H₂O₂ on cell growth and alkaline phosphatase activity, as well as on the expression of various osteoblast differentiation genes. The addition of Rp-cyclic 3',5'-hydrogen phosphorothioate adenosine triethylammonium salt (a cyclic 3',5'-adenosine monophosphate antagonist) and calphostin C (a protein kinase C inhibitor), or a PTH type 1 receptor antagonist, abrogated the effects of N-terminal PTHrP, whereas protein phosphatase 1 (an Src kinase activity inhibitor), SU1498 (a vascular endothelial growth factor receptor 2 inhibitor), or an anti osteostatin antiserum, inhibited the effects of C-terminal PTHrP.

Conclusion

These findings indicate that the antioxidant properties of PTHrP act through its N- and C-terminal domains and provide novel insights into the osteogenic action of PTHrP.

Cite this article: *Bone Joint Res* 2018;7:58–68.

Keywords: Parathyroid hormone-related protein, Osteostatin, Antioxidant activity

Article focus

- Oxidative stress is associated with bone loss.
- We assessed *in vitro* the putative antioxidant properties of the osteogenic parathyroid hormone-related protein (PTHrP) and their ability to modulate osteoblastic function.

Key messages

- PTHrP displays antioxidative stress activity in mouse and human osteoblastic cells.
- PTHrP (1-37) and PTHrP (107-111) (osteostatin) counteract the decrease of osteoblastic function triggered by oxidative stress.

- N- and C-terminal domains of PTHrP exhibit similar antioxidative stress features through different signalling mechanisms in osteoblastic cells.

Strengths and limitations

- PTHrP preserves osteoblastic function in an *in vitro* oxidative environment that further supports the putative use of PTHrP peptides as osteoporosis therapy.
- Caution should be taken when translating these *in vitro* results to an *in vivo* scenario.

Introduction

It is widely accepted that bone mass in humans starts to decline between the second and third decades of life, and this has been attributed to an increase in oxidative stress.^{1,2} Compelling evidence indicates that oxidative stress is a major cause of the ageing process, and that it occurs as the result of an imbalance between the production of reactive oxygen species (ROS) and the molecular defence mechanisms that control ROS, such as antioxidant enzymes catalase (CAT), superoxide dismutase (SOD), glutathione peroxidase (GPx), and antioxidant compounds (glutathione, among others).^{3,4} It has been reported that age-related conditions that are associated with bone derangement, such as post-menopausal oestrogen depletion and diabetes mellitus, produce an increase of ROS.^{5,6} The expression of ROS inhibiting molecules, namely the enzymes SOD⁷ and CAT,⁸ as well as factors that induce cell cycle arrest in response to excessive oxidative stress (such as growth arrest DNA damage 45 protein),⁹ can be regulated by forkhead box protein O (FOXO) transcription factors, which are essential to bone integrity.¹⁰ In fact, it has recently been demonstrated that knocking down SOD results in bone deterioration in mice.¹¹ In humans, an augmented oxidative stress has been traced to decreased bone mineral density.^{12,13} The mechanisms by which oxidative stress may impair bone formation are complex and involve DNA damage,¹⁴ lipid peroxidation,¹⁵ protein carbonylation,¹⁶ inhibition of Wnt pathway activation,¹⁷ decreased osteoblast proliferation¹⁸ and differentiation,^{19,20} and increased osteoblast apoptosis.²¹

Parathyroid hormone (PTH)-related protein (PTHrP) is abundantly expressed in bone, where it performs an important role in bone formation and remodelling; similarly to PTH, intermittent administration of PTHrP displays anabolic actions in rodents and/or humans.²² In fact, the N-terminal region of PTHrP shows homology with the same region of PTH and interacts with the common PTH type 1 receptor (PTH1R), which is a class II G protein-coupled receptor. PTH binding to PTH1R produces the activation of protein kinase A (PKA) by cyclic 3',5'-adenosine monophosphate (cAMP) and phospholipase C.²³ On the other hand, the PTH-unrelated C-terminal tail of PTHrP contains the 107-111 epitope (named osteostatin), which does not interact with the parathyroid hormone 1 receptor (PTH1R) but can apparently signal through opening voltage-sensitive calcium channels and protein kinase C (PKC) activation in osteoblastic cells.²⁴ It has recently been shown that osteostatin may transactivate vascular endothelial growth factor receptor 2 (VEGFR2) to promote osteoblastic function through an Src kinase-mediated mechanism.²⁵

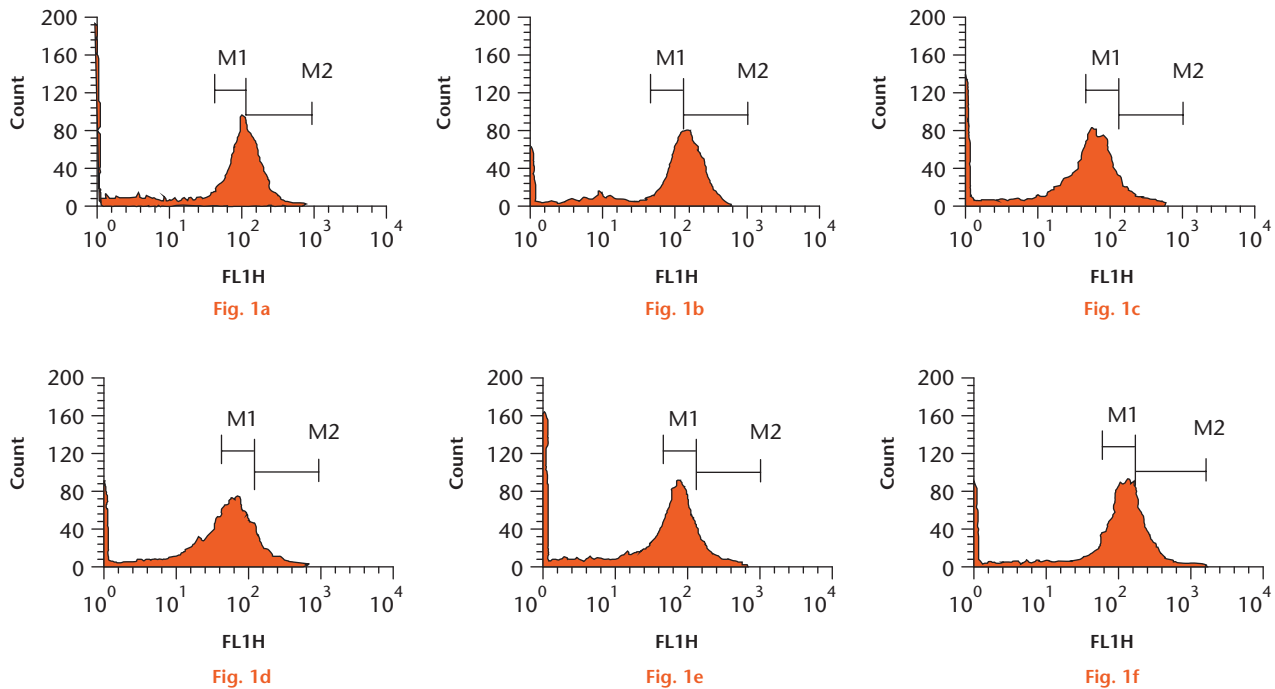
Recent data have disclosed the impact of the antioxidative stress properties of PTH on its bone anabolic action in aged mice.²⁶ In this regard, we recently reported that PTHrP (1-36) and PTHrP (107-139) were able to prevent the inhibitory effect of oxidative stress on the Wnt pathway activation in mouse mesenchymal C3H10T1/2 cells,

suggesting their antioxidant potential.²⁷ The aim of the present study was to determine the antioxidant properties of both N- and C-terminal domains of PTHrP in murine osteoblastic MC3T3-E1 cells and human osteoblastic cells (hOBs). Regarding the latter domain, we tested both the native fragment PTHrP (107-139) and osteostatin, both of which have a simple structure that would make them attractive agents for promoting bone formation and bone regeneration.²⁸⁻³² The impact of the antioxidant properties of these PTHrP peptides on their ability to affect murine and hOB function has also been explored in this study.

Materials and Methods

Cells and reagents. Previously well-characterized osteoblastic MC3T3-E1-subclon 4 cells (CRL-2593; American Type Culture Collection, Manassas, Virginia), showing high mineralization capacity under differentiation conditions, were used. These cells have been used in previous studies evaluating several osteogenic actions of PTH and PTHrP.^{28,29,33,34} Primary hOBs were obtained from trabecular bone explants from two osteoarthritic patients undergoing total knee arthroplasty surgery, as previously reported.^{22,28,29,35-37} Briefly, hOBs were cultured from bone slices with Dulbecco's modified Eagle medium (MEM; Thermo Fisher Scientific, Waltham, Massachusetts) containing 20% heat-inactivated fetal bovine serum (FBS), 2 mM glutamine and 100 U/ml of penicillin/streptomycin, and experiments were carried out using cells at the third passage. The Ethics Committee for Clinical Research at Instituto de Investigación Sanitaria-Fundación Jiménez Díaz, Madrid, Spain approved the protocol, and written informed consent from the patients was granted.

MC3T3-E1 cells were grown in α -MEM with 10% FBS and antibiotics were made up of 1% penicillin/streptomycin (standard medium) in a humidified atmosphere of 5% CO₂ at 37°C. When present, PTH (1-34) (Sigma-Aldrich, St Louis, Missouri), PTHrP (1-37), PTHrP (107-139), and osteostatin (Bachem AG, Bubendorf, Switzerland), depending on the type of experiment (detailed in each case), were added at 100 nM to the cell culture. This dose has demonstrated osteogenic capacity in previous studies using PTHrP (1-37) and osteostatin.^{27,29,34,38} In order to evaluate gene expression changes as described below, the PTH1R antagonist (Asn10, Leu11, D-Trp12) PTHrP (7-34) amide (PTHrP 7-34), at 100 nM, or neutralizing rabbit polyclonal antiserum C7 recognizing the osteostatin epitope in the entire PTHrP molecule, at 1:100 dilution,³⁹ were added together with PTHrP (1-37) or osteostatin, respectively. CAT (Sigma-Aldrich), at 200 U/ml, was used as an antioxidant control. In alkaline phosphatase (ALP) activity and viability assays, we used the PKA inhibitor, adenosine 3',5'-cyclic monophosphorothioate, and Rp-isomer (Rp-cyclic 3',5'-hydrogen phosphorothioate adenosine triethylammonium salt (Rp-cAMPs)) (Santa Cruz Biotechnology Inc., Santa Cruz, California), at 25 μ M; the PKC inhibitor, calphostin C (CalpC) (Calbiochem Corp., La



Oxidative stress induced by hydrogen peroxide (H_2O_2) can be prevented by N- and C-terminal parathyroid hormone (PTH) and PTH-related protein (PTHrP) peptides in osteoblastic cells. Cells were exposed to $200\mu M H_2O_2$ following pretreatment with each PTHrP peptide or PTH (1-34) (100 nM) or control. Reactive oxygen species levels were measured by 2',7'-dichloro fluorescein diacetate (DCF) fluorescence. Representative flow cytometry images for a) control, b) H_2O_2 , c) PTH + H_2O_2 , d) PTHrP (1-37) + H_2O_2 , e) PTHrP (107-139) + H_2O_2 , and f) osteostatin + H_2O_2 . M1 and M2 denote the two areas used to quantify increment in fluorescence.

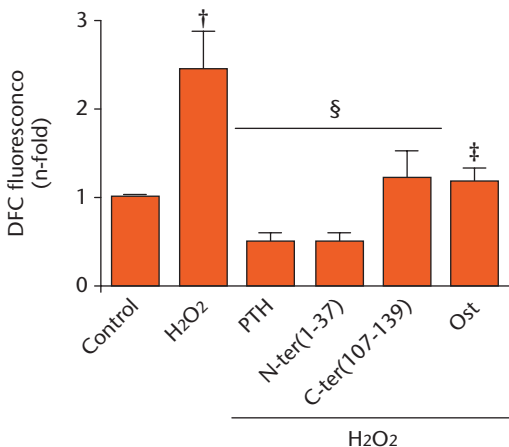


Fig. 2

Representative flow cytometry quantification. † $p < 0.01$ versus control; ‡ $p < 0.05$ versus H_2O_2 treatment; § $p < 0.01$ versus H_2O_2 treatment. Data are represented by mean \pm standard error of the mean (SEM). Kruskal–Wallis test followed by Dunn’s *post hoc* test. N-ter(1-37), C-ter(107-139), and Ost denote parathyroid hormone-related protein (1-37), parathyroid hormone-related protein (107-139), and osteostatin, respectively.

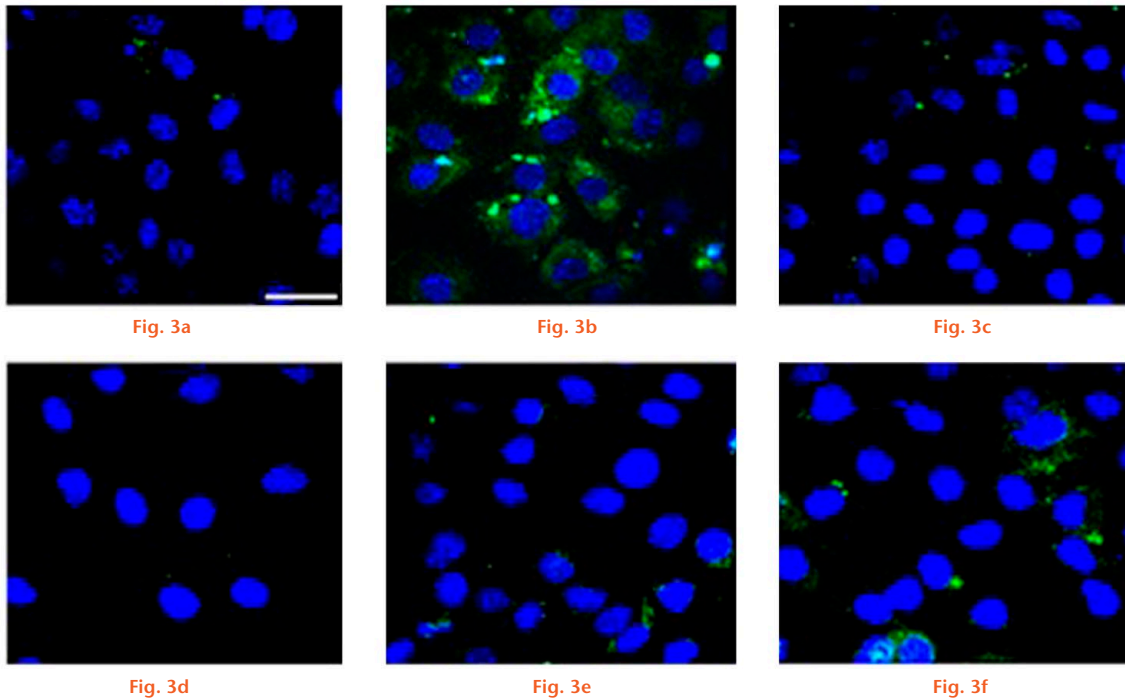
Jolla, California), at 250 nM ; or the Src kinase inhibitor PP-1 (Calbiochem Corp.) and VEGFR2 phosphorylation inhibitor SU1498 (Sigma-Aldrich), each at $10\mu M$, all of them added 30 minutes prior to the tested peptides.

ROS level determination. ROS were measured by evaluating the fluorescence increment of 2',7'-dichlorofluorescein diacetate (DCF) dye reacting with strong oxidants such as cell peroxides, as previously described.^{40,41} Briefly, a final concentration of $10\mu M$ DCF was added to subconfluent

cells (10000 cells/cm^2 to 20000 cells/cm^2) in a FBS-depleted medium for 15 minutes at $37^\circ C$. After extensive washing with phosphate-buffered saline (PBS), pH 7.4, cells were incubated for another 15 minutes, followed by treatment with the tested peptides at 100 nM for ten minutes in standard medium. After removing this medium, cells were washed with PBS followed by an addition of $200\mu M$ hydrogen peroxide (H_2O_2) for ten minutes in a FBS-depleted medium and then trypsinized, measuring the increment of fluorescence in a FACSCalibur flow cytometer (BD Biosciences, Franklin Lakes, New Jersey).

Confocal experiments were also performed following the same protocol described above for DCF loading and peptide and H_2O_2 treatments. Cells were subsequently fixed with methanol including the DNA fluorescent dye 4',6-diamidino-2-phenylindole dihydrochloride (1 mg/ml) for ten minutes, mounted in FluorSave reagent (Calbiochem Corp.) and examined using a Leica DM IRB confocal microscope (Leica, Wetzlar, Germany).

FOXO-luciferase (luc) assay. Subconfluent MC3T3-E1 cells were transfected with a mixture of $1\mu g$ of FOXO-luc reporter plasmid and 5 ng of a renilla coding plasmid (Promega Corp., Fitchburg, Wisconsin) (transfection control) using X-tremeGENE 9 DNA Transfection Reagent (Roche Diagnostics, Indianapolis, Indiana), following the manufacturer’s instructions. After transfection, cells were treated with the peptides (each at 100 nM) for one hour in standard medium and then washed with PBS before the addition of $100\mu M H_2O_2$, followed by an overnight incubation in 1% FBS-containing medium at $37^\circ C$.



Confocal microscopy images of MC3T3-E1 cells for a) control, b) H_2O_2 , c) parathyroid hormone (PTH) + H_2O_2 , d) PTH-related protein (1-37) + H_2O_2 , e) PTH-related protein (107-139) + H_2O_2 , and f) osteostatin + H_2O . The white bar denotes 75 μ m.

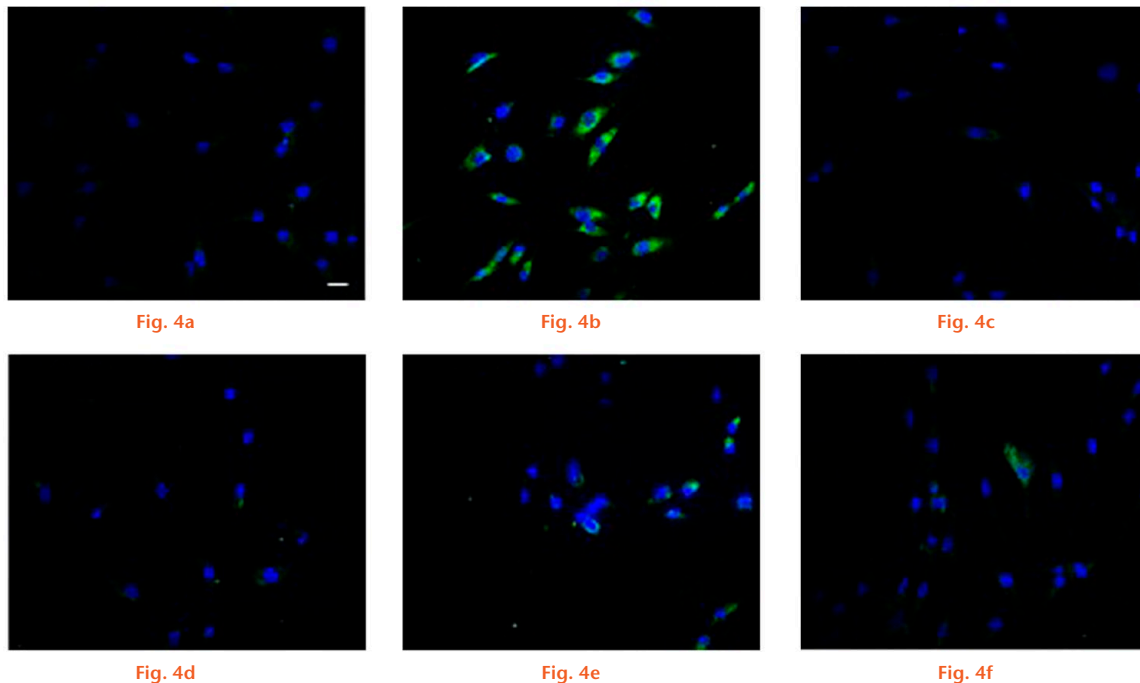
Thereafter, cells were homogenized with a lysis buffer, and luciferase and renilla activities were quantified with a dual luciferase kit (Promega Corp.), following the manufacturer's instructions, using the FB12 tube luminometer (Berthold Technologies GmbH & Co. KG, Bad Wildbad, Germany). Renilla activity values were used to normalize the luciferase values.

Malondialdehyde (MDA) assay. Lipid peroxidation levels were determined by measuring the formation of MDA using a commercial kit (BioVision, Inc., Mountain View, California) per the manufacturer's instructions. Briefly, MC3T3-E1 cells and hOBs (2×10^6 cells) were pretreated with PTHrP (1-37), PTHrP (107-139), osteostatin or PTH (1-34), each at 100 nM, for ten minutes in a serum-depleted medium. Cells were then washed three times with PBS and treated with 200 μ M H_2O_2 for 24 hours, followed by centrifugation at $500 \times g$ for five minutes. The pellets were then washed three times with PBS. Pellets were subsequently resuspended in 300 μ l of lysis buffer, as supplied by the kit, with 3 μ l butylated hydroxytoluene (0.1 mM), sonicated, and centrifuged ($13\,000 \times g$ for ten minutes). The supernatants (200 μ l) from each sample were added to 600 μ l of thiobarbituric acid and incubated in a water bath at 95°C for 60 minutes. Samples were then ice-cooled for ten minutes and 200 μ l (from each 800 μ l of reaction mixture) was placed into a 96-well microplate for measuring absorbance at 532 nm. The MDA supplied in the kit was used as standard and MDA levels were determined by comparing the absorbance of samples with that of the standard controls. The protein concentration of the samples was measured with bicinchoninic

acid protein assay (Sigma-Aldrich), using bovine serum albumin as standard. Results were expressed as nmols of MDA per mg of protein.

Caspase-3 assay. Subconfluent cells were serum-depleted overnight prior to incubation with the different peptides tested (each at 100 nM) for one hour in FBS-depleted medium. After washing the cells with PBS, 100 μ M H_2O_2 was added for two, six, and 24 hours in the latter medium. Caspase-3 activity was analyzed using the CaspACE Assay System (Promega) following the manufacturer's instructions. In brief, cell extracts obtained in lysis buffer were submitted to three freeze-and-thaw cycles and then centrifuged at 15 000 g at 4°C. Supernatants were then incubated with the substrate Ac-DEVD-p-nitroaniline (Sigma-Aldrich) for four hours at 37°C, and caspase-3 activity was determined by measuring absorbance at 405 nm. Caspase activity was expressed as pmol p-nitroaniline/h/ μ g protein (measured as described above).

Cell proliferation. Cells were seeded at 3000 cells/cm² in 96-well plates. After 24 hours, cells were treated with each tested peptide, at 100 nM, or CAT (an antioxidant control) at 200 U/ml, for one hour in standard medium. After washing with PBS, 200 μ M H_2O_2 was added for one hour in FBS-depleted medium. The medium was then replaced with the standard medium. This procedure was repeated after 48 hours and 24 hours after this repetition we proceeded to measure cell proliferation (a total five days since assay onset). At this time, cell proliferation was determined by the addition of resazurin salt solution⁴² (Sigma-Aldrich), at 10 μ g/ml. After four hours, absorbance was measured at both 540 nm and 630 nm.



Confocal microscopy images of human osteoblastic cells for a) control, b) H_2O_2 , c) parathyroid hormone (PTH) + H_2O_2 , d) PTH-related protein (1-37) + H_2O_2 , e) PTH-related protein (107-139) + H_2O_2 , and f) osteostatin + H_2O_2 . The white bar denotes 20 μm .

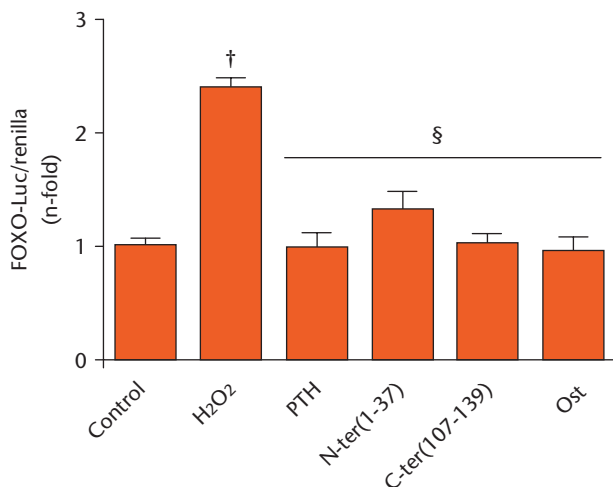


Fig. 5

Forkhead box protein O (FOXO) activity in MC3T3-E1 cells was measured with a FOXO-luciferase plasmid. Bars represent the mean \pm standard error of the mean (SEM) of three independent experiments performed in triplicate. $\dagger p < 0.01$ versus control; $\S p < 0.01$ versus H_2O_2 treatment. Kruskal–Wallis test followed by Dunn's *post hoc* test. N-ter(1-37), C-ter(107-139), and Ost denote parathyroid hormone-related protein (1-37), parathyroid hormone-related protein (107-139), and osteostatin, respectively.

The percentage difference in cell growth between treated and control cells was calculated using the following equation: $[(O2 \times A1) - (O1 \times A2) / (O2 \times P1) - (O1 \times P2)] \times 100$, where O1 and O2 are the molar extinction coefficients of oxidized resazurin salt at 540 nm and 630 nm, respectively; A1 and A2 are the absorbance of treated cells at 540 nm and 630 nm, respectively; and P1 and P2

correspond to the absorbance of control cells (cells without treatment) at 540 nm and 630 nm, respectively.

Cell viability. Subconfluent MC3T3-E1 cells were pre-treated for 30 minutes with the inhibitors prior to the addition of PTHrP peptides for 30 minutes in standard medium. Controls were not pretreated. The cells were then washed with PBS and incubated with 200 μM H_2O_2 for six hours in either serum-depleted or standard medium (to control for endogenous growth factors in FBS). After treatment, nonadherent cells were collected and pooled with adherent cells (following trypsinization), and cell viability was assessed by trypan blue exclusion, as previously described.^{36,43} Nonviable cells exhibiting intracellular trypan blue staining and total cell numbers were counted to calculate the percentage of cell viability in each case.

ALP activity assay. Subconfluent MC3T3-E1 cells and hOBs were preincubated with the different inhibitors for 30 minutes, subsequently followed by the addition of the tested PTHrP peptides, each at 100 nM for one hour in standard medium and 200 μM of H_2O_2 for two hours in FBS-depleted medium. The FBS-depleted medium was then replaced with standard medium and cells were incubated for a further 24 hours. ALP activity was measured in cell extracts obtained with PBS and 0.1% Triton X-100 (Sigma-Aldrich) using p-nitrophenyl phosphate as substrate, as previously described.²⁸ ALP activity was normalized to cell protein content determined as described in MDA and Caspase assays.

Quantitative real-time polymerase chain reaction (PCR). Subconfluent MC3T3-E1 cells were treated as described for the ALP activity assay. Following treatment, cell total RNA was extracted with TRIzol (Thermo Fisher Scientific,

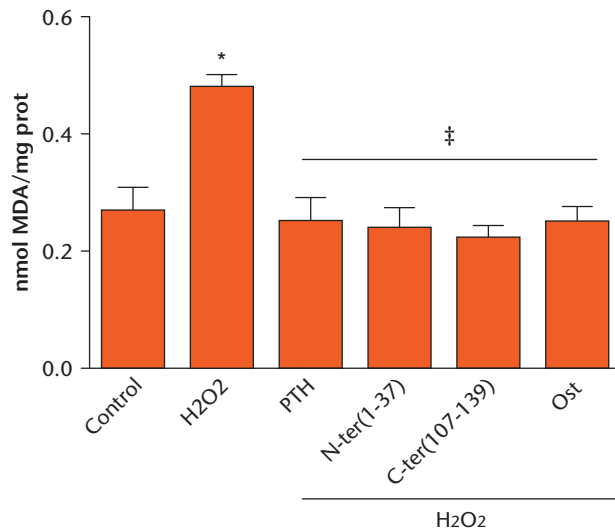


Fig. 6a

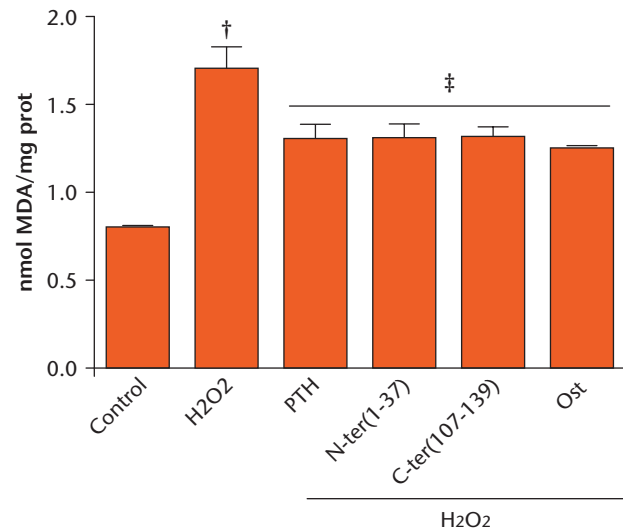


Fig. 6b

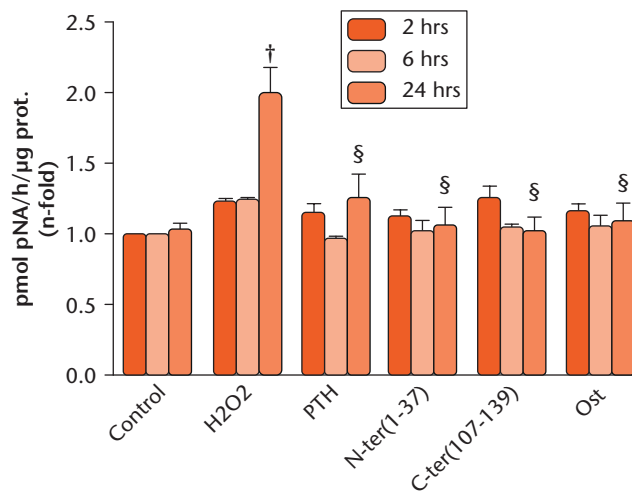


Fig. 6c

Parathyroid hormone (PTH) and both N- and C-terminal PTH-related protein (PTHrP) peptides prevented the increase in malondialdehyde (MDA) levels and caspase-3 activation induced by H_2O_2 in osteoblastic cells. Cells were pretreated with the different peptides at 100 nM followed by H_2O_2 (200 μ M) for a) and b) ten minutes, or c) two to 24 hours. Changes in MDA levels in a) MC3T3-E1 cells and b) human osteoblastic cells, and in c) caspase-3 activity in MC3T3-E1 cells, are shown. Data are mean \pm standard error of the mean (SEM) of three independent experiments performed at least in triplicate. * $p < 0.05$ versus corresponding time control; † $p < 0.01$ versus corresponding time control; ‡ $p < 0.05$ versus H_2O_2 at the corresponding time; § $p < 0.01$ versus H_2O_2 at the corresponding time. Kruskal–Wallis test followed by Dunn's *post hoc* test. N-ter(1-37), C-ter(107-139), and Ost denote PTHrP (1-37), PTHrP (107-139), and osteostatin, respectively.

Waltham, Massachusetts). Synthesis of complementary DNA (cDNA) was performed using the high-capacity cDNA reverse transcription kit following the manufacturer's instructions (Applied Biosystems, Grand Island, New York). A quantitative real-time PCR was performed in an ABI PRISM 7500 system (Applied Biosystems). TaqMan minor groove binder probes (Applied Biosystems, Assay-by-Design) were obtained for amplification of the following genes: runt-related transcription factor 2 (Runx2), osterix (Osx) and ALP using Premix ex-Taq polymerase (Takara Bio Inc., Otsu, Japan). The messenger RNA (mRNA) copy numbers were calculated for each sample using the cycle threshold value and normalized against 18S ribosomal RNA, as previously reported.^{44,45} Results were expressed as

n-fold mRNA values versus corresponding values in non-treated control cells.

Statistical analysis. Results are expressed as mean \pm standard error of the mean (SEM) throughout the text. Differences among groups were analyzed by the Kruskal–Wallis test followed by Dunn's *post hoc* test and $p < 0.05$ was considered significant. Statistical analysis was performed with SPSS v21 software (IBM Corp., Armonk, New York).

Results

Both N- and C-terminal PTHrP peptides counteract H_2O_2 -induced oxidative stress in osteoblastic cells. First, we aimed to explore whether N- and C-terminal PTHrP peptides might be able to prevent ROS production by the

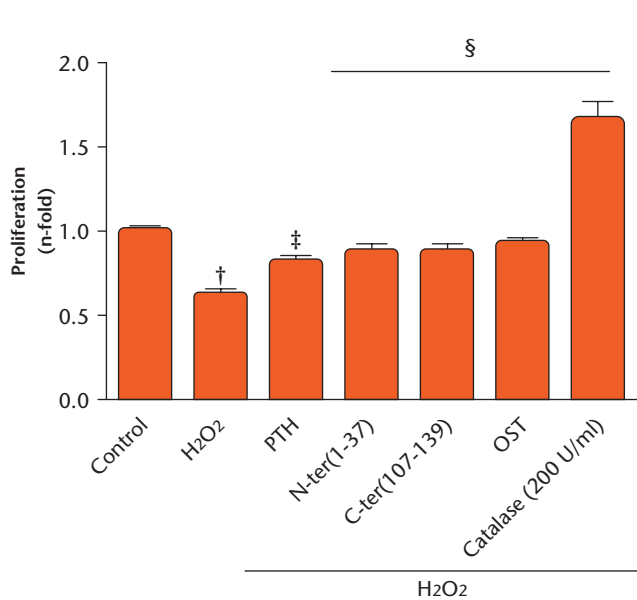


Fig. 7a

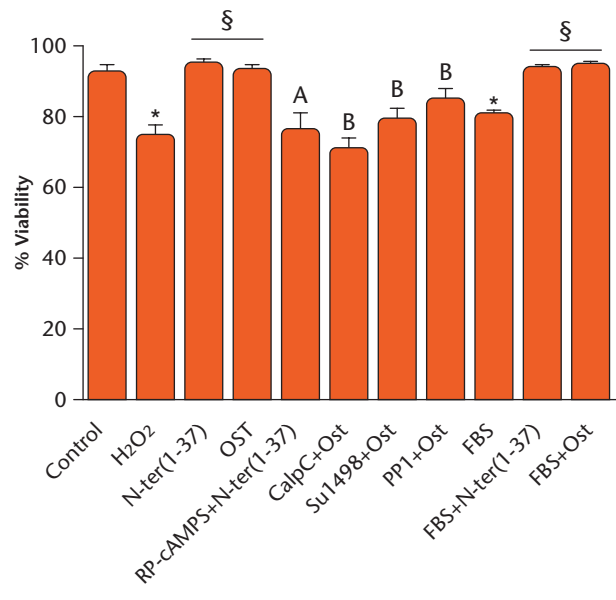


Fig. 7b

Parathyroid hormone (PTH) and both N- and C-terminal PTH-related protein (PTHrP) peptides counteract the deleterious effects of H₂O₂ on MC3T3-E1 cell growth. Cells were preincubated with different inhibitors for 30 minutes: Rp-cyclic 3',5'-hydrogen phosphorothioate adenosine triethylammonium salt (Rp-cAMPS; 25 μM), protein phosphatase 1 and Su1498 (5 μM) or calphostin C (CalpC) (250 nM), and then treated with PTHrP peptides (100 nM) before exposure to H₂O₂. Control cells were not treated. a) For calculation of cell proliferation, cell growth percentage values in treated samples were expressed as n-fold versus control (normalized to 1). Catalase (200 U/ml) was used as an antioxidant control. b) Cell viability was expressed as the percentage of viable cells over total cells. Data are mean ± standard error of the mean (SEM) of three independent experiments performed at least in triplicate. *p < 0.05 versus control; †p < 0.01 versus control; ‡p < 0.05 versus H₂O₂; §p < 0.01 versus H₂O₂; probability associated with comparison A (^p) < 0.05 versus H₂O₂ + N-ter(1-37); probability associated with comparison B (°p) < 0.05 versus H₂O₂ + Ost. Kruskal–Wallis test followed by Dunn's *post hoc* test. N-ter(1-37), C-ter(107-139) and Ost denote PTHrP (1-37), PTHrP (107-139), and osteostatin, respectively. FBS, fetal bovine serum.

prominent oxidative stress-related agent H₂O₂ in osteoblastic cells. Short exposure (ten minutes) of MC3T3-E1 cells to 200 μM H₂O₂ produced a significant (p < 0.01) increase in intracellular ROS (Figs 1 and 2). However, this increase was prevented by each N- or C-terminal PTHrP peptide tested or PTH (1-34) (a positive control) (each at 100 nM). Further confirmation of the capacity of these peptides to impair oxidative stress was obtained by using confocal microscopy to assess H₂O₂-induced DCF fluorescence changes in MC3T3-E1 cells and in hOBs (Figs 3 and 4).

It has been demonstrated that increased cell ROS lead to an augmented FOXO transcriptional activity.^{46,47} Thus, we next examined the changes in this activity elicited by H₂O₂ and the possible modulatory effects of the different peptides evaluated in MC3T3-E1 cells. We found that preincubation with either PTHrP peptide or PTH (1-34) abrogated the oxidant-related effect of H₂O₂ in these cells (Fig. 5).

Oxidative stress induces different kinds of cellular damage, which impairs regular cell function.¹ Thus, we next analyzed the changes in MDA levels induced by H₂O₂ as an oxidative stress damage marker and the possible modulatory action of the different PTHrP peptides. As expected, this oxidative agent increased MDA levels, which were normalized by pretreating MC3T3-E1 cells and hOBs with the PTHrP peptides or PTH (1-34) (Figs 6a and b). It has been demonstrated that oxidative stress

triggers an apoptotic cascade resulting in caspase activation.²¹ We found that caspase-3 activity increased significantly after 24 hours of exposure to H₂O₂, and all of the peptides tested were similarly effective in normalizing this activity in these cells (Fig. 6c).

Protective effects of both N- and C-terminal PTHrP peptides against the deleterious effects of H₂O₂ on osteoblastic cell function. Osteoblast growth has been shown to be altered negatively by oxidative stress.^{18,19} This prompted us to examine whether PTHrP would prevent the negative effects of a short exposure (one hour) to H₂O₂ during MC3T3-E1 cell growth for five days. Indeed, we showed a diminished cell proliferation with H₂O₂ treatment, which was similarly compensated for by both N- and C-terminal PTHrP peptides (Fig. 7a). Of note, CAT (used as an antioxidant control) produced a dramatic stimulation for cell proliferation, suggesting that basal H₂O₂ levels keep proliferation under control in these cells. In addition, we found that either the N- or C-terminal PTHrP domain could counteract the inhibitory effect of acute exposure of MC3T3-E1 cells to H₂O₂ in the presence or absence of FBS on cell viability (Fig. 7b).

We also aimed to explore the putative changes elicited by short exposure to H₂O₂ on various osteoblast differentiation markers and the modulatory effect of PTHrP peptides in MC3T3-E1 cells and hOBs. This oxidant was found to reduce ALP activity in both osteoblastic cell

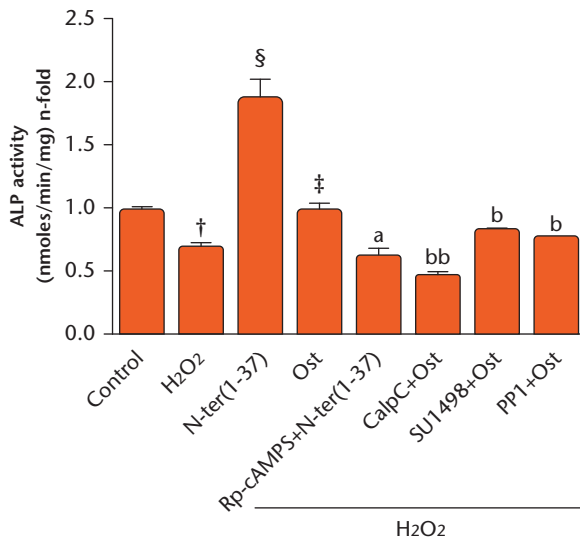


Fig. 8a

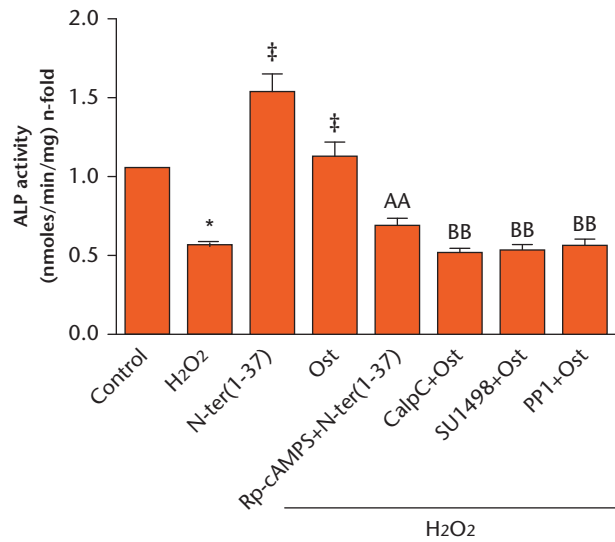


Fig. 8b

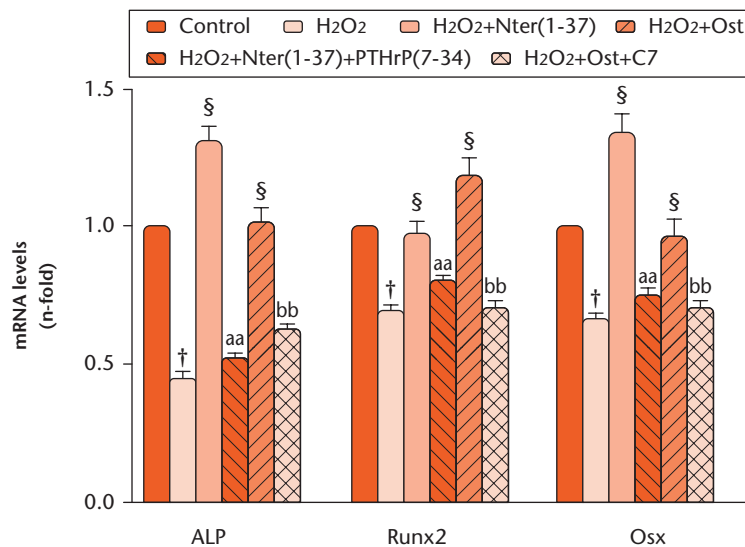


Fig. 8c

Parathyroid hormone (PTH) and both N- and C-terminal PTH-related protein (PTHrP) peptides counteract the negative effects of H₂O₂ on osteoblastic cell differentiation. a) MC3T3-E1 cells and b) human osteoblastic cells were preincubated or not with different inhibitors, as described in the legend for Figure 7, and then treated or not (control) with the PTHrP peptides (100 nM) before exposure to H₂O₂. Alkaline phosphatase (ALP) activity was expressed as n-fold over control (mean \pm standard error of the mean (SEM): 2.6 nmoles/min/mg (SEM 0.5) and 4.3 nmoles/min/mg (SEM 0.22) protein for MC3T3-E1 cells and human osteoblastic cells, respectively). c) MC3T3-E1 cells were pre treated with the PTHrP peptides in the presence or absence of the antagonist PTHrP (7-34) or the anti-osteostatin antiserum C7 before addition of H₂O₂. Changes in gene expression of ALP, runt-related transcription factor 2 (Runx2) and osterix (Osx) were analyzed in cell total RNA isolates by quantitative polymerase chain reaction. †p < 0.01 versus control; ‡p < 0.05 versus H₂O₂; §p < 0.01 versus H₂O₂; probability associated with comparison A (†p) < 0.05; probability associated with comparison AA (AAp) < 0.01 versus H₂O₂ + N-ter(1-37); probability associated with comparison B (‡p) < 0.05; comparison associated with comparison BB (BBp) < 0.01 versus H₂O₂ + Ost. N-ter(1-37), C-ter(107-139) and Ost denote PTHrP (1-37), PTHrP (107-139) and osteostatin, respectively. Rp-cAMPS, Rp-cyclic 3',5'-hydrogen phosphorothioate adenosine triethylammonium salt; CalpC, calphostin C; mRNA, messenger RNA.

types (Figs 8a and b), as well as the gene expression of ALP, Runx2, and Osx in MC3T3-E1 cells (Fig. 8c); these deleterious effects were prevented by pretreating these cells with each PTHrP peptide tested (Figs 8a to c).

As a specificity control of each PTHrP peptide action in this setting, we used several inhibitors or antagonists. Thus, we found that Rp-cAMPS (a PKA inhibitor) inhibited the ability of PTHrP (1-37) to preserve cell viability and ALP activity upon exposure to H₂O₂ in MC3T3-E1 cells,

whereas CalpC (a PKC inhibitor), protein phosphatase 1 (Src activation inhibitor) or SU1498 (VEGFR2 activation inhibitor) abrogated such ability of osteostatin to restore ALP activity upon oxidant treatment in these cells (Figs 7b, 8a, and 8b). In addition, PTHrP (7-34) (a PTHR1 antagonist) and anti-osteostatin antiserum C7 inhibited the positive effects of PTHrP (1-37) and osteostatin, respectively, on osteoblast differentiation-related genes in these cells following H₂O₂ treatment (Fig. 8c).

Discussion

Oestrogen depletion has traditionally been considered the hallmark of the pathogenesis of involutional osteoporosis,⁴⁸ but age-related factors intrinsic to bone, mainly oxidative stress, appear also to contribute to bone loss in this condition.^{1,2} In this regard, the recent finding that intermittent PTH, currently the only bone anabolic therapy, may function, at least partially, through reducing oxidative stress in aged bone²⁶ provides insight into the mechanisms and possible treatment options for bone loss. However, the use of antioxidants alone or in combination with PTH presents several drawbacks. Thus, common antioxidants such as N-acetyl cysteine and CAT produce a decrease in ROS levels, but can also decrease osteoblastogenesis by blocking Wnt pathway activation,⁴⁹ thereby inhibiting β -catenin-dependent transcription of osteogenic genes.²⁶ In addition, antioxidants have anti-osteoclastic features that would inhibit bone remodelling.²⁶

Previous studies have shown the ability of N- and C-terminal PTHrP peptides to promote cell growth and osteoblast differentiation in MC3T3-E1 cells and other osteoblastic cell preparations. Studies on these proteins have also reported their osteogenic properties *in vivo* in high oxidative stress-related conditions, namely diabetes mellitus and ovariectomized mice.^{24,25,27-29,32,34-36,39} Very recently, the osteoregenerative features of both PTHrP (1-37) and osteostatin have been reported *in vivo* in an ageing rat model with diabetes mellitus, although only indirect evidence for the antioxidant capacities of these peptides was provided.⁵⁰

In this *in vitro* study, we disclose the antioxidant capacity of both N- and C-terminal domains of PTHrP in well-characterized osteoblastic cells. To induce oxidative stress, we used H₂O₂ at concentrations widely used in previous studies.^{18,38,51} ROS elevation can impair bone formation by interaction with the Wnt/ β -catenin pathway.¹⁷ Thus, ROS-mediated activation of FOXO transcription factors diverts β -catenin from the promoter regions of genes involved in proliferation and differentiation of cells of the osteoblastic lineage, impairing these cellular programmes.⁵² Our data show that these PTHrP peptides were able to prevent the H₂O₂-induced generation of cell ROS in both murine osteoblastic cells and hOBs, and accordingly, the increase in FOXO transcriptional activity as demonstrated by a FOXO-luc reporter assay in the former cells. This is consistent with recent results showing the ability of PTHrP to increase Wnt/ β -catenin signalling in osteoblastic cells exposed to high glucose concentrations, another oxidative stress-related scenario.³³ Oxidative stress also triggers cellular damage and apoptosis through caspase activation.^{21,53} Here we show that pretreatment with these peptides decreased lipid peroxidation and blocked caspase-3 activation, thus protecting MC3T3-E1 cells from apoptosis in both osteoblastic cell types used.

It has been reported previously that oxidative stress impairs osteoblast function.^{5,17-19,21,51} In the present study, we report that short exposure (one to six hours) of MC3T3-E1 cells to H₂O₂ significantly decreased cell proliferation and viability by approximately 30%. This decrease is moderate compared with previous data in the same osteoblast cell line, although previous studies used prolonged exposure to the oxidant in a FBS-containing medium and/or higher oxidant concentration than that used herein.^{18,19} In addition, ALP enzymatic activity and mRNA levels, as well as gene expression of other well-known osteoblast differentiation markers, were all diminished by acute exposure to H₂O₂, and this was also prevented by pretreatment with both PTHrP peptides in MC3T3-E1 cells and hOBs.

Previous reports have shown the important role of the cAMP/PKA pathway in the anabolic actions elicited by the homologous N-terminal domains of PTH and PTHrP.^{22,24,25,35,36} This fact was confirmed by using a PKA inhibitor in the present oxidative stress scenario. In addition, specific inhibitors of PKC and Src-dependent VEGFR2 activation inhibited the protective/restoring role of osteostatin in viability and ALP activity, supporting the notion that both pathways play a major role in its osteogenic actions.^{24,25,36} Our results thus further emphasize the involvement of distinct signalling pathways triggered by both the N- and C-terminal PTHrP domains in osteoblasts.

Taken together, the present data indicate that both N- and C-terminal domains of PTHrP display various antioxidant features in both murine osteoblastic cells and hOBs. However, we understand that this is an *in vitro* study and caution should be taken when translating our results to an *in vivo* scenario. Even so, these findings provide novel insights that add support to the generally accepted use of PTHrP peptides as osteoporosis therapy.

References

1. **Manolagas SC.** From estrogen-centric to aging and oxidative stress: a revised perspective of the pathogenesis of osteoporosis. *Endocr Rev* 2010;31:266-300.
2. **Khosla S, Melton LJ III, Riggs BL.** The unitary model for estrogen deficiency and the pathogenesis of osteoporosis: is a revision needed? *J Bone Miner Res* 2011;26:441-451.
3. **De la Fuente M, Miquel J.** An update of the oxidation-inflammation theory of aging: the involvement of the immune system in oxi-inflamm-aging. *Curr Pharm Des* 2009;15:3003-3026.
4. **Harman D.** Aging: a theory based on free radical and radiation chemistry. *J Gerontol* 1956;11:298-300.
5. **Almeida M, Han L, Martin-Millan M, et al.** Skeletal involution by age-associated oxidative stress and its acceleration by loss of sex steroids. *J Biol Chem* 2007;282:27285-27297.
6. **Hamada Y, Kitazawa S, Kitazawa R, et al.** Histomorphometric analysis of diabetic osteopenia in streptozotocin-induced diabetic mice: a possible role of oxidative stress. *Bone* 2007;40:1408-1414.
7. **Kops GJPL, Dansen TB, Polderman PE, et al.** Forkhead transcription factor FOXO3a protects quiescent cells from oxidative stress. *Nature* 2002;419:316-321.
8. **Nemoto S, Finkel T.** Redox regulation of forkhead proteins through a p66shc-dependent signaling pathway. *Science* 2002;295:2450-2452.

9. Tran H, Brunet A, Grenier JM, et al. DNA repair pathway stimulated by the forkhead transcription factor FOXO3a through the Gadd45 protein. *Science* 2002;296:530-534.
10. Ambrogini E, Almeida M, Martin-Millan M, et al. FoxO-mediated defense against oxidative stress in osteoblasts is indispensable for skeletal homeostasis in mice. *Cell Metab* 2010;11:136-146.
11. Nojiri H, Saita Y, Morikawa D, et al. Cytoplasmic superoxide causes bone fragility owing to low-turnover osteoporosis and impaired collagen cross-linking. *J Bone Miner Res* 2011;26:2682-2694.
12. Cervellati C, Bonaccorsi G, Cremonini E, et al. Oxidative stress and bone resorption interplay as a possible trigger for postmenopausal osteoporosis. *Biomed Res Int* 2014;2014:569563.
13. Basu S, Michaëlsson K, Olofsson H, Johansson S, Melhus H. Association between oxidative stress and bone mineral density. *Biochem Biophys Res Commun* 2001;288:275-279.
14. Cooke MS, Evans MD, Dizdaroglu M, Lunec J. Oxidative DNA damage: mechanisms, mutation, and disease. *FASEB J* 2003;17:1195-1214.
15. Jacob KD, Noren Hooten N, Trzeciak AR, Evans MK. Markers of oxidant stress that are clinically relevant in aging and age-related disease. *Mech Ageing Dev* 2013;134:139-157.
16. Stadtman ER, Levine RL. Free radical-mediated oxidation of free amino acids and amino acid residues in proteins. *Amino Acids* 2003;25:207-218.
17. Almeida M, Han L, Martin-Millan M, O'Brien CA, Manolagas SC. Oxidative stress antagonizes Wnt signaling in osteoblast precursors by diverting beta-catenin from T cell factor- to forkhead box O-mediated transcription. *J Biol Chem* 2007;282:27298-27305.
18. Li M, Zhao L, Liu J, et al. Hydrogen peroxide induces G2 cell cycle arrest and inhibits cell proliferation in osteoblasts. *Anat Rec (Hoboken)* 2009;292:1107-1113.
19. Mody N, Parhami F, Sarafian TA, Demer LL. Oxidative stress modulates osteoblastic differentiation of vascular and bone cells. *Free Radic Biol Med* 2001;31:509-519.
20. Bai XC, Lu D, Bai J, et al. Oxidative stress inhibits osteoblastic differentiation of bone cells by ERK and NF-kappaB. *Biochem Biophys Res Commun* 2004;314:197-207.
21. Almeida M, Han L, Ambrogini E, Bartell SM, Manolagas SC. Oxidative stress stimulates apoptosis and activates NF-kappaB in osteoblastic cells via a PKCbeta/p66shc signaling cascade: counter regulation by estrogens or androgens. *Mol Endocrinol* 2010;24:2030-2037.
22. Esbrit P, Alcaraz MJ. Current perspectives on parathyroid hormone (PTH) and PTH-related protein (PTHrP) as bone anabolic therapies. *Biochem Pharmacol* 2013;85:1417-1423.
23. Sneddon WB, Magyar CE, Willick GE, et al. Ligand-selective dissociation of activation and internalization of the parathyroid hormone (PTH) receptor: conditional efficacy of PTH peptide fragments. *Endocrinology* 2004;145:2815-2823.
24. Valín A, Guillén C, Esbrit P. C-terminal parathyroid hormone-related protein (PTHrP) (107-139) stimulates intracellular Ca(2+) through a receptor different from the type 1 PTH/PTHrP receptor in osteoblastic osteosarcoma UMR 106 cells. *Endocrinology* 2001;142:2752-2759.
25. García-Martín A, Acitores A, Maycas M, Villanueva-Peñacarrillo ML, Esbrit P. Src kinases mediate VEGFR2 transactivation by the osteostatin domain of PTHrP to modulate osteoblastic function. *J Cell Biochem* 2013;114:1404-1413.
26. Jilka RL, Almeida M, Ambrogini E, et al. Decreased oxidative stress and greater bone anabolism in the aged, when compared to the young, murine skeleton with parathyroid hormone administration. *Ageing Cell* 2010;9:851-867.
27. de Castro LF, Lozano D, Portal-Núñez S, et al. Comparison of the skeletal effects induced by daily administration of PTHrP (1-36) and PTHrP (107-139) to ovariectomized mice. *J Cell Physiol* 2012;227:1752-1760.
28. Lozano D, Sánchez-Salcedo S, Portal-Núñez S, et al. Parathyroid hormone-related protein (107-111) improves the bone regeneration potential of gelatin-glutaraldehyde biopolymer-coated hydroxyapatite. *Acta Biomater* 2014;10:3307-3316.
29. Lozano D, Feito MJ, Portal-Núñez S, et al. Osteostatin improves the osteogenic activity of fibroblast growth factor-2 immobilized in Si-doped hydroxyapatite in osteoblastic cells. *Acta Biomater* 2012;8:2770-2777.
30. Trejo CG, Lozano D, Manzano M, et al. The osteoinductive properties of mesoporous silicate coated with osteostatin in a rabbit femur cavity defect model. *Biomaterials* 2010;31:8564-8573.
31. Manzano M, Lozano D, Arcos D, et al. Comparison of the osteoblastic activity conferred on Si-doped hydroxyapatite scaffolds by different osteostatin coatings. *Acta Biomater* 2011;7:3555-3562.
32. Lozano D, Manzano M, Doadrio JC, et al. Osteostatin-loaded bioceramics stimulate osteoblastic growth and differentiation. *Acta Biomater* 2010;6:797-803.
33. López-Herradón A, Portal-Núñez S, García-Martín A, et al. Inhibition of the canonical Wnt pathway by high glucose can be reversed by parathyroid hormone-related protein in osteoblastic cells. *J Cell Biochem* 2013;114:1908-1916.
34. Lozano D, de Castro LF, Dapia S, et al. Role of parathyroid hormone-related protein in the decreased osteoblast function in diabetes-related osteopenia. *Endocrinology* 2009;150:2027-2035.
35. de Gortázar AR, Alonso V, Alvarez-Arroyo MV, Esbrit P. Transient exposure to PTHrP (107-139) exerts anabolic effects through vascular endothelial growth factor receptor 2 in human osteoblastic cells in vitro. *Calcif Tissue Int* 2006;79:360-369.
36. Alonso V, de Gortázar AR, Ardura JA, et al. Parathyroid hormone-related protein (107-139) increases human osteoblastic cell survival by activation of vascular endothelial growth factor receptor-2. *J Cell Physiol* 2008;217:717-727.
37. Villalvilla A, García-Martín A, Largo R, et al. The adipokine lipocalin-2 in the context of the osteoarthritic osteochondral junction. *Sci Rep* 2016;6:29243.
38. Ardura JA, Portal-Núñez S, Castellón-Calvo I, et al. Parathyroid hormone-related protein protects osteoblastic cells from oxidative stress by activation of MKP1 phosphatase. *J Cell Physiol* 2017;232:785-796.
39. Lozano D, Fernández-de-Castro L, Portal-Núñez S, et al. The C-terminal fragment of parathyroid hormone-related peptide promotes bone formation in diabetic mice with low-turnover osteopaenia. *Br J Pharmacol* 2011;162:1424-1438.
40. Peiró C, Lafuente N, Matesanz N, et al. High glucose induces cell death of cultured human aortic smooth muscle cells through the formation of hydrogen peroxide. *Br J Pharmacol* 2001;133:967-974.
41. Huang X, Frenkel K, Klein CB, Costa M. Nickel induces increased oxidants in intact cultured mammalian cells as detected by dichlorofluorescein fluorescence. *Toxicol Appl Pharmacol* 1993;120:29-36.
42. O'Brien J, Wilson I, Orton T, Pognan F. Investigation of the Alamar Blue (resazurin) fluorescent dye for the assessment of mammalian cell cytotoxicity. *Eur J Biochem* 2000;267:5421-5426.
43. Alonso V, Pérez-Martínez FC, Calahorra FJ, Esbrit P. Phytoestrogen modulation of bone-related cytokines and its impact on cell viability in human prostate cancer cells. *Life Sci* 2009;85:421-430.
44. Portal-Núñez S, Lozano D, de Castro LF, et al. Alterations of the Wnt/beta-catenin pathway and its target genes for the N- and C-terminal domains of parathyroid hormone-related protein in bone from diabetic mice. *FEBS Lett* 2010;584:3095-3100.
45. Livak KJ, Schmittgen TD. Analysis of relative gene expression data using real-time quantitative PCR and the 2(-Delta Delta C(T)) Method. *Methods* 2001;25:402-408.
46. van der Horst A, de Vries-Smits AMM, Brenkman AB, et al. FOXO4 transcriptional activity is regulated by monoubiquitination and USP7/HAUSP. *Nat Cell Biol* 2006;8:1064-1073.
47. Furuyama T, Nakazawa T, Nakano I, Mori N. Identification of the differential distribution patterns of mRNAs and consensus binding sequences for mouse DAF-16 homologues. *Biochem J* 2000;349:629-634.
48. Riggs BL, Khosla S, Melton LJ III. A unitary model for involutional osteoporosis: rigidity deficiency causes both type I and type II osteoporosis in postmenopausal women and contributes to bone loss in aging men. *J Bone Miner Res* 1998;13:763-773.
49. Funato Y, Michiue T, Asashima M, Miki H. The thioredoxin-related redox-regulating protein nucleoredoxin inhibits Wnt-beta-catenin signalling through dishevelled. *Nat Cell Biol* 2006;8:501-508.
50. Ardura JA, Portal-Núñez S, Lozano D, et al. Local delivery of parathyroid hormone-related protein-derived peptides coated onto a hydroxyapatite-based implant enhances bone regeneration in old and diabetic rats. *J Biomed Mater Res A* 2016;104:2060-2070.
51. Fatokun AA, Stone TW, Smith RA. Responses of differentiated MC3T3-E1 osteoblast-like cells to reactive oxygen species. *Eur J Pharmacol* 2008;587:35-41.
52. Hoogeboom D, Essers MAG, Polderman PE, et al. Interaction of FOXO with beta-catenin inhibits beta-catenin/T cell factor activity. *J Biol Chem* 2008;283:9224-9230.
53. Almeida M, Ambrogini E, Han L, Manolagas SC, Jilka RL. Increased lipid oxidation causes oxidative stress, increased peroxisome proliferator-activated receptor-gamma expression, and diminished pro-osteogenic Wnt signaling in the skeleton. *J Biol Chem* 2009;284:27438-27448.

Funding Statement

■ This work has been funded by grants from the Fundación para la Investigación Ósea y Metabolismo Mineral-FEIOMM and the Instituto de Salud Carlos III (PI11/00449, PI15/00340, PI1600065, RD12/0043/0029, RD12/0043/0008 and RD12/0043/0018.). J. A. Ardua, D. Lozano, and S. Portal-Núñez are recipients of postdoctoral contracts from the Ministerio de Economía y Competitividad, Juan de la Cierva program [CI-2011-09548, FPI-2013-17268, and RETICEF [FEDER “una manera de hacer Europa” (RD12/0043/0008)].

Author Contribution

■ S. Portal-Núñez: Designing the study, Data acquisition, Statistical analysis, Writing the manuscript, Final approval of the manuscript.
■ J. A. Ardua: Designing the study, Data acquisition, Writing the manuscript, Statistical analysis.
■ D. Lozano: Data acquisition, Writing the manuscript, Statistical analysis.

■ I. Martínez de Toda: Data acquisition.
■ M. De la Fuente: Designing the study, Revising the manuscript, Final approval of the manuscript.
■ G. Herrero-Beaumont: Revising the manuscript, Financial support.
■ R. Largo: Revising the manuscript, Financial support.
■ P. Esbrit: Study direction, Designing the study, Writing and revising the manuscript, Financial support.

Conflicts of Interest Statement

■ None declared

© 2018 Portal-Núñez et al. This is an open-access article distributed under the terms of the Creative Commons Attribution licence (CC-BY-NC), which permits unrestricted use, distribution, and reproduction in any medium, but not for commercial gain, provided the original author and source are credited.